

Rhizaria in the oligotrophic ocean exhibit clear temporal and vertical variability.

Alex Barth^{*1,2}, Leocadio Blanco-Berical³, Rod Johnson³ and Joshua Stone¹

1. University of South Carolina, Biological Sciences, 700 Sumter St 401, Columbia, SC 29208
2. University of Texas at Austin, Marine Science Institute, 750 Channel Drive, Port Aransas, Texas, USA
3. Arizona State University, School of Ocean Futures, Bermuda Institute of Ocean Sciences 17 Biological Station, St Georges, GE 01

Abstract

Recently studies have shown that Rhizaria, a super-group of marine protists, have a large role in pelagic ecosystems. They are unique in that they construct mineral tests out of silica, calcium carbonate, or strontium sulfate. As a consequence, Rhizaria can have large impacts on the ocean's cycling of carbon and other elements. However, less is known about Rhizaria ecology or their role in the pelagic food-web. Some taxa, like certain Radiolarians, are mixotrophic, hosting algal symbionts. While other taxa are flux-feeders or even predatory carnivores. Some prior research has suggested that Rhizaria will partition vertically in the water column, likely due to different trophic strategies. However, very few studies have investigated their populations over extended periods of time. In this study, we present data investigating Rhizaria abundance and vertical distribution from over a year of monthly cruises in the Sargasso Sea. This study represents the first quantification of Rhizaria throughout the mesopelagic zone in an oligotrophic system for an extended period of time. We use this data to investigate the hypothesis that Rhizaria taxonomic groups will partition due to trophic mode. We also investigate how their abundance varies in accordance with environmental parameters. Rhizaria abundance was quantified using an Underwater Vision Profiler (UVP5), an in-situ imaging device. Ultimately, we show that different Rhizaria taxa will have unique vertical distribution patterns. Models relating their abundance to environmental parameters have mixed results, yet particle concentration is a common predictive variable, supporting the importance of heterotrophy amongst many taxa.

² Introduction

³ Rhizaria are an extremely diverse super-group of single-celled organisms which occupy a wide range of
⁴ habitats. Planktonic Rhizaria include Foraminifera, Radiolaria (including Acantharea and Collodaria) and
⁵ Phaeodaria, all of which are observed throughout the global ocean (Biard *et al.*, 2016; Laget *et al.*, 2024)
⁶. While the taxonomy of these organisms has recently undergone several reclassifications (Biard, 2022b),
⁷ their presence in ocean ecosystems has been long known to oceanographers. Some of the earliest records
⁸ of their existence are from oceanographic expeditions in the 19th century (Haekel, 1887). Rhizaria are
⁹ unique members of the plankton and protist community because they can reach large sizes (up to several
¹⁰ mm in diameter) and they construct intricate mineral skeletons out of either silica, strontium, or calcium
¹¹ carbonate (Kimoto, 2015; Nakamura and Suzuki, 2015; Suzuki and Not, 2015; Biard, 2022b). Despite their
¹² noticeable morphology and global distribution, Rhizaria were largely understudied throughout the 20th
¹³ century. Fragile organisms like Rhizaria are difficult to adequately study because they can be destroyed
¹⁴ through standard zooplankton sampling techniques and preserve poorly. A number of studies in the late
¹⁵ 1900s did employ alternative techniques to quantify Rhizaria including diaphragm pumps (Michaels, 1988)
¹⁶ or blue-water SCUBA collections (Caron and Be, 1984; Bijma *et al.*, 1990; Caron *et al.*, 1995). However, the
¹⁷ bulk of Rhizaria research was constrained to sediment traps or paleontological studies of sediment (Takahashi
¹⁸ *et al.*, 1983; Boltovskoy *et al.*, 1993).

¹⁹ Recently, the advent of molecular techniques and *in situ* imaging tools have ignited a renewed focus on
²⁰ Rhizaria in pelagic ecosystems (Caron, 2016). Molecular tools have shed light on Rhizaria taxonomy (Biard,
²¹ 2022b), distribution (Blanco-Bercial, 2020; Sogawa *et al.*, 2022), ecology (Decelle *et al.*, 2012; Nakamura *et*
²² *al.*, 2023), biogeochemical roles (Gutierrez-Rodriguez *et al.*, 2019; Laget *et al.*, 2024), and metabolism (Cohen
²³ *et al.*, 2023). Yet, despite the excellent taxonomic resolution provided by molecular approaches, they do not
²⁴ provide a truly quantitative metric for estimating Rhizaria abundance or biomass. *In situ* imaging tools

however, offer the ability to observe organisms in the natural state and quantify their abundance (Ohman, 2019; Barth and Stone, 2024). Biard *et al.* (2016) utilized *in situ* imaging at a global scale to suggest large ($>500\mu\text{m}$ diameter) Rhizaria were substantial contributors to the ocean carbon standing stock. While more recent calculations suggest lower carbon contribution (Laget *et al.*, 2024), Rhizaria nonetheless have substantial influences on biogeochemical cycling. This influence is due to their unique mineral skeletons and ability to repackage small particles into larger, fast sinking ones (Ikenoue *et al.*, 2019). Thus, some Rhizaria may play substantial roles in ocean export through their interception of sinking particles (Stukel *et al.*, 2018; Laget *et al.*, 2024). However, Rhizaria ecology is poorly understood (Biard, 2022b) and their ecological roles are likely more than diverse than simple particle interception.

The ecological role of Rhizaria in plankton communities is complicated due to the fact different taxa can exhibit very different trophic modes. Many Rhizaria are strictly heterotrophic (Biard, 2022b), yet their feeding modes can be quite varied. Phaeodaria are largely thought to be flux-feeders, collecting and feeding on sinking particles (Gowing, 1989). Alternatively, Retaria can be either exclusively heterotrophic or mixotrophic, utilizing photosynthetic algal symbionts (Anderson, 2014; Decelle *et al.*, 2015). Mixotrophic Foraminifera host a variety of endosymbiont partners (Lee, 2006; Decelle *et al.*, 2015), which are thought to support early and adult life stages and significantly contribute to total primary productivity (Kimoto, 2015). Still, Foraminifera are omnivorous, possibly even predominately carnivorous, with several studies suggesting that they can be effective predators (Anderson and Bé, 1976; Gaskell *et al.*, 2019), mainly consuming live copepods (Caron and Be, 1984). Radiolaria have several lineages, many of which host symbionts (Biard, 2022a). Amongst Radiolaria, arguably the most widespread are Collodaria who can be either large solitary cells or form massive colonies, up to several meters in length (Swanberg and Anderson, 1981). All known Collodaria species host dinoflagellate symbionts (Biard, 2022a) and can contribute substantially to primary productivity, particularly in oligotrophic ocean regions (Caron *et al.*, 1995; Dennett *et al.*, 2002). This

48 Collodaria-symbiont association has been suggested as a reason for their high abundances throughout the
49 photic zone of oligotrophic environments globally (Biard *et al.*, 2016, 2017). A few Acantharea (Radiolaria
50 order) clades host algal symbionts (Decelle *et al.*, 2012; Biard, 2022a), notably with two clades forming an
51 exclusive relationship with *Phaeocystis*. However, globally, Acantharea are less abundant than Collodaria
52 (Biard, 2022b) and contribute less to total primary productivity (Michaels *et al.*, 1995). This may be due to
53 the fact several clades of Acantharea are cyst-forming and strictly heterotrophs (Decelle *et al.*, 2013; Biard,
54 2022a). Furthermore, Mars Brisbin *et al.* (2020) documented apparent predation behavior in Acantharea
55 near the surface, suggesting that there may be a larger reliance on carnivory.

56 Given the high abundances, yet diverse trophic strategies found among Rhizaria taxa, it is reasonable to
57 expect some form of niche partitioning. A number of studies do suggest evidence for vertical zonation
58 between Rhizaria groups according to various trophic strategies. Taxon-specific studies of Radiolaria suggest
59 they may be restricted to the euphotic zone (Michaels, 1988; Boltovskoy, 2017). Although some studies
60 report Acantharea in deeper waters (Decelle *et al.*, 2013; Gutiérrez-Rodríguez *et al.*, 2022), Phaeodaria,
61 alternatively, are generally found beyond depths where light can sustain photosynthesis, but they can feed
62 on sinking particles (Stukel *et al.*, 2018; Laget *et al.*, 2024). In an imaging-based study of the whole Rhizaria
63 community, Biard and Ohman (2020) noted clear patterns in vertical zonation which largely corresponded
64 to different trophic roles. Protists communities, including Rhizaria, have been described to partition along
65 autotroph-mixotroph-heterotroph gradients with increasing depth in the water column (Blanco-Bercial *et*
66 *al.*, 2022; Laget *et al.*, 2024). Yet, few studies have made direct attempts to relate Rhizaria abundances to
67 environmental factors (Biard and Ohman, 2020). In part, this is due to the fact few studies have been able
68 to sample Rhizaria in the same location over a consistent timeframe (Michaels, 1988; Boltovskoy *et al.*, 1993;
69 Michaels *et al.*, 1995; Hull *et al.*, 2011; Gutiérrez-Rodríguez *et al.*, 2022). Furthermore, very few studies
70 have utilized *in situ* imaging, arguably the best method for quantifying Rhizaria, to consistently throughout

71 the full mesopelagic (Laget *et al.*, 2024) . Given this lack of information, there are many unknowns with
72 respect to Rhizaria ecology, seasonality and phenology across different groups.

73 In this study, we present a comprehensive assessment of large Rhizaria abundance measured for over a year
74 from regularly occurring cruises at monthly intervals. We utilized an *in situ* imaging approach to facilitate
75 abundance calculations. With this dataset, we address two critical aims. 1) Quantifying of large Rhizaria
76 throughout the epipelagic (0-200m) and mesopelagic (200-1000m) over the course of an annual cycle. These
77 data were collected in the Sargasso Sea, and represents the first study of its kind in an oligotrophic sys-
78 tem; and 2) We aim to test the hypothesis that Rhizaria exhibit niche partitioning according to trophic
79 roles. This hypothesis has several implications, including vertical zonation, as seen in prior studies, but also
80 that environmental variables related to trophic strategy will explain abundance patterns. Specifically, au-
81 totrophic/mixotrophic taxa will correspond to variables related to autotrophy (chl-a concentration, primary
82 productivity, local DO maxima) and other rhizaria will correspond to factors which promote heterotrophy
83 (particle concentration, flux, and local DO minima).

84 Methods

85 Oceanographic sampling

86 Data were collected in collaboration with the Bermuda Atlantic Time-series Study (Michaels and Knap, 1996;
87 Lomas *et al.*, 2013) on board the R/V Atlantic Explorer. Cruises were conducted at approximately monthly
88 intervals. Rhizaria individuals were sampled using the Underwater Vision Profiler 5 (UVP) (Picheral *et al.*,
89 2010). The UVP5 is an in-situ camera used to capture plankton and particle images and has been well
90 established to accurately quantify large Rhizaria abundance (Biard *et al.*, 2016; Stukel *et al.*, 2018; Stukel *et*
91 *al.*, 2019; Biard and Ohman, 2020; Barth and Stone, 2022; Drago *et al.*, 2022; Llopis Monferrer *et al.*, 2022;

92 Panaïotis *et al.*, 2023). The UVP5 was mounted to the sampling rosette and collected data autonomously on
93 routine casts, from which only the downcast data are utilized. The UVP5 was deployed from June-September
94 2019 then from October 2020 - January 2022, during which time the BATS region was sampled for 3-5 days
95 at monthly intervals (see sampling details in Supplemental Table 1). Casts were filtered to only include data
96 collected in the BATS region, far offshore of Bermuda in the Sargasso Sea (approximately $31.0^{\circ}N$ - $32.5^{\circ}N$,
97 $64.25^{\circ}W$ - $63^{\circ}W$; Supplemental Figure 1). In general, casts extended to either 200m, 500m, or 1200m deep,
98 with a few extended into the bathypelagic (4500m). However, Rhizaria were only typically found in large
99 abundances throughout the epipelagic and mesopelagic zones. As such, we limit this study to results from
100 the upper 1000m of the water column.

101 A variety of biotic and abiotic data were collected during each BATS cruise. The UVP5 provided particle
102 count data at a high-frequency from each cast. Particle concentration, as a proxy for prey field (Whitmore
103 and Ohman, 2021), was calculated from this data for all particles $184\mu m$ - $900\mu m$. The lower size range
104 was set by what could be reliably sampled by the UVP5's pixel resolution ($>2px$; 0.092mm per pixel) and
105 the upper size range was set to below the size of observable Rhizaria yet large enough to be inclusive of
106 particles on which some Rhizaria may feed. For each UVP cast supporting continuous profiles of the CTD
107 parameters salinity, temperature, and auxiliary CTD channels; Dissolved Oxygen (DO), *in situ* chlorophyll
108 fluorescence were measured at 24Hz using the BATS CTD package. On select casts, Niskin bottles were
109 used to collect bacterial abundance estimates (via epifluorescence microscopy) as well as measure inorganic
110 nutrients (NO_3 , and Si as silicate/silicic acid) at discrete depths. On each cruise, flux estimates of total
111 mass, organic carbon, and nitrogen were also collected using sediment traps; in the present study we utilized
112 flux to the mesopelagic as the flux at 200m. Also primary productivity was estimated through measuring ^{14}C
113 uptake rates from *in situ* incubations. For full descriptions of the BATS sampling program and methods,
114 see Knap *et al.* (1997) and Lomas *et al.* (2013) for a review. Additionally, data can be viewed online

115 (<https://bats.bios.asu.edu/bats-data/>).

116 Environmental data were processed to match the format of the Rhizaria abundance estimates (see below).

117 CTD data were collected at higher frequency than the UVP (24Hz vs 15Hz respectively), so these data were

118 averaged within matching bins to the UVP5 data. Data from Niskin bottles were first linearly interpolated

119 in depth at 1m resolution then time averaged over the cruise, then subsequently averaged into matching

120 bins as the UVP5 data. Primary productivity estimates were depth integrated throughout the euphotic zone

121 (0-140m).

122 Rhizaria imaging processing and abundance quantification

123 Individual vignettes of Rhizaria images were identified using the classification platform EcoTaxa (Picheral

124 *et al.*). Data were pre-sorted utilizing a random-forest classifier and pre-trained learning set. Taxonomic

125 classification were done based on morphological parameters measured in Zooprocess (Gorsky *et al.*, 2010),

126 which includes parameters such as major axis, equivalent spherical diameter (ESD), and grey values. While

127 there are sparse taxonomic guides for *in situ* images of Rhizaria, identification largely relied on descrip-

128 tions in (Nakamura and Suzuki, 2015; Suzuki and Not, 2015; and Biard and Ohman, 2020). Using

129 the aforementioned sources and publicly available EcoTaxa projects, we constructed a guide accessible

130 at: [https://thealexbarth.github.io/media//Project_Items/Oligotrophic_Community/ecotaxa_UVP-guide-](https://thealexbarth.github.io/media//Project_Items/Oligotrophic_Community/ecotaxa_UVP-guide-stone-lab.pdf)

131 [stone-lab.pdf](https://thealexbarth.github.io/media//Project_Items/Oligotrophic_Community/ecotaxa_UVP-guide-stone-lab.pdf). Broadly, Rhizaria were classified as Foraminifera, Radiolaria (Acantharea or Collodaria), or

132 as a variety of Phaeodaria families (Figure 1). When identification could not be confidently made between

133 a few candidate taxa, a less specific label was used. As a result, we have data from “unidentified Rhizaria”,

134 which typically were vignettes not distinguishable between Aulacanthidae or Acantharea or “unidentified

135 Phaeodaria”, which are clearly Phaeodaria but not distinguishable into a family.

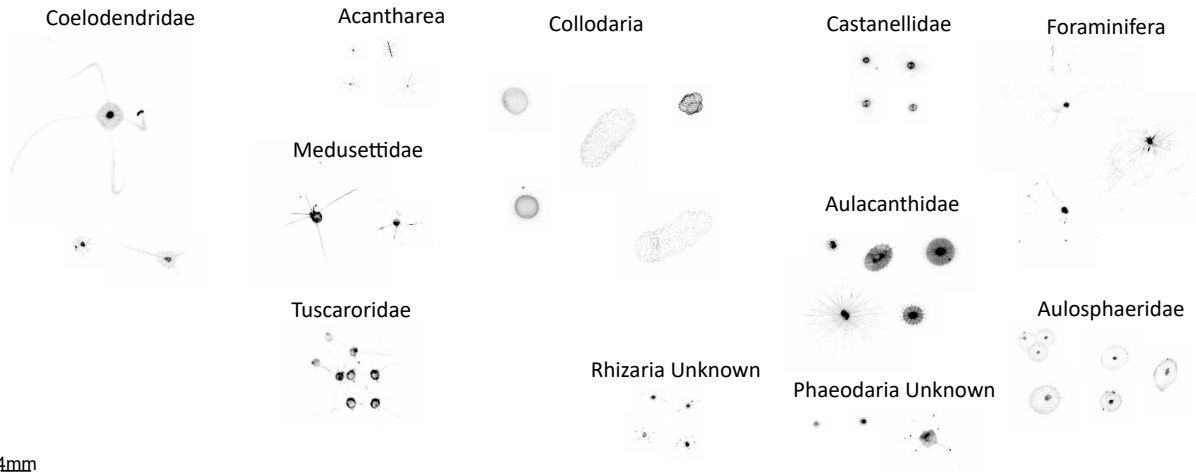


Figure 1: Example images of different Rhizaria taxa as collected by UVP5 imaging. 4mm scale bar shown in lower right. All vignettes are same scale

136 The UVP5 samples at \sim 15Hz rate as it descends the water column and records the exact position of each
 137 particle larger than $600\mu m$ (ESD). However, identified rhizaria ranged from a $934\mu m$ ESD Aulacanthidae
 138 cell to a Collodarian colony over 10mm in diameter. To confirm that the UVP5 was sampling adequately
 139 across all size ranges, a normalized biomass size spectrum (NBSS) slope was constructed to identify a
 140 drop-off which would indicate poor-sampling at the small size range (Lombard *et al.*, 2019; Barth and
 141 Stone, 2024). However, it was evident from this analysis that all size ranges were adequately sampled across
 142 the size range (Supplemental Figure 2) so no data were excluded. The UVP5 reports the exact depth at
 143 which a particle is recorded, however to estimate abundance, observations must be binned over fixed depth
 144 intervals. Our deployments had variable descent depths and speeds with more casts descending to 500m than
 145 1000m and descents quicker through the epipelagic than the mesopelagic (see Barth and Stone (2022) for an
 146 extended discussion of UVP5 data processing). For the present study, Rhizaria abundances were estimated
 147 in 25m vertical bins, which offer a moderate sampling volume per bin (average $0.948m^3$ in the epipelagic
 148 and $0.589m^3$ in the mesopelagic; Supplemental Table 1) while still maintaining ecologically relevant widths.

149 However, concentrations in a 25m bin would need to be greater than 2.428 ind. m^{-3} and 3.912 ind. m^{-3} ,
150 in the epipelagic and mesopelagic respectively, to fall below a 10% non-detection risk (Benfield *et al.*, 1996;
151 Barth and Stone, 2024). Because we typically observed many Rhizaria taxa below these concentrations, we
152 present the 25m binned data to visualize broad-scale average distributions. For quantifying and modelling
153 Rhizaria abundances, we present integrated abundance estimates, with each cast. Due to the variable descent
154 depths of the UVP, data are categorized as epipelagic (0-200m), upper mesopelagic (200-500m), and lower
155 mesopelagic (500-1000m). The average sampling volume integrated through these regions were $7.59m^2$,
156 $7.06m^2$, and $11.77m^2$, with non-detection thresholds at 0.30 ind. m^{-2} , 0.33 ind. m^{-2} , and 0.20 ind. m^{-2}
157 respectively. All UVP data processing was done using the `EcotaxaTools` package in R (Barth 2023).

158 Modelling environmental controls of Rhizaria abundance

159 Generalized Additive Models (GAMs) were used to assess the relationship between integrated Rhizaria abun-
160 dance and different environmental factors. GAMs offer the ability to model non-linear and non-monotonic
161 relationships, which can be particularly useful in assessing ecological relationships (Wood, 2017) and have
162 been successfully applied to Rhizaria ecology (Biard and Ohman, 2020). The `mgcv` package (Wood, 2001)
163 was used to construct models relating environmental parameters to each taxonomic group's integrated abun-
164 dance estimates from each cast. To select the most parsimonious model for each analysis, a backwards
165 step-wise approach was taken. First, a full model was fit using any term which may be ecologically relevant.
166 Terms were fit using maximum likelihood with a double penalty approach on unnecessary smooths (Marra
167 and Wood, 2011). The smoothness parameter was restricted ($k = 6$) to prevent over fitting the models.
168 Then, the full model was checked for concurvity (a metric indicating high parameter relatedness in GAMs).
169 If two terms had a high concurvity value (>0.8), then two alternative models were constructed each leaving
170 out one of the related terms. The more parsimonious model of these two was selected using AIC. Once

171 concurvity of terms was reduced, then the model was subjected to the backwards step-wise procedure. At
172 each iteration, the model term with the lowest F score (least statistically significant) was removed. This
173 was repeated until all model terms were statistically significant or the R^2_{adj} was substantially reduced. Mod-
174 els were fit for each water column region; epipelagic, upper mesopelagic, and lower mesopelagic. In cases
175 where observations were too sparse for a given taxonomic grouping, models were not run. All code, full
176 models, and model selection tools are available in open-source scripts, as well as intermediate data products
177 at <https://github.com/TheAlexBarth/RhizariaSeasonality>.

178 Results

179 Environmental Variability

180 While the environmental conditions were generally low in variation and oligotrophic, there is considerable
181 influence from deep winter-mixing and summer stratification as well as secondary influences from mesoscale
182 eddies which result in spatiotemporal heterogeneity (McGillicuddy *et al.*, 1998; Lomas *et al.*, 2013). Vari-
183 ability in the water column structure was visible during the study period (Figure 2). This is best evidenced
184 through the temperature profiles; In the late summer and early fall there was a stratified water column with
185 high temperatures in the surface (<75m) (Figure 2A) and slightly elevated salinity (Figure 2B). This warm,
186 stratified period appeared more intense during the few months sampled in 2019. In 2021, we observed the
187 stratified layer slowly dissipated into the winter months following mixed layer entrainment. There was a
188 consistent oxygen minimum zone (OMZ) located at about 800m deep (Figure 2C). February 2021 saw a
189 notable downwelling event, likely due to a passing anti-cyclonic eddy which impacted the local region during
190 early 2021. During this phase, warmer, oxic water was significantly depressed deeper into the mesopelagic.
191 This process was reversed in the spring months (March, April) primary due to the interaction of convective

192 mixing and the passing of a strong cyclonic eddy resulting in a deep cold mixed layer. Primary production
193 was highest during the spring mixing period, evidenced both by *in situ* fluorescence (Figure 2D) and produc-
194 tivity incubation experiments (Figure 3A). Originating near the surface, the productivity peak moved deeper
195 throughout the spring and declined into the summer (Figure 2D). However, there was a notable, yet smaller
196 productivity bump in the late summer and early fall (Figure 3A) which occurred deeper in the epipelagic
197 (Figure 2D). The particle concentration ($184\mu m - 900\mu m$) was closely coupled to chlorophyll-a patterns.

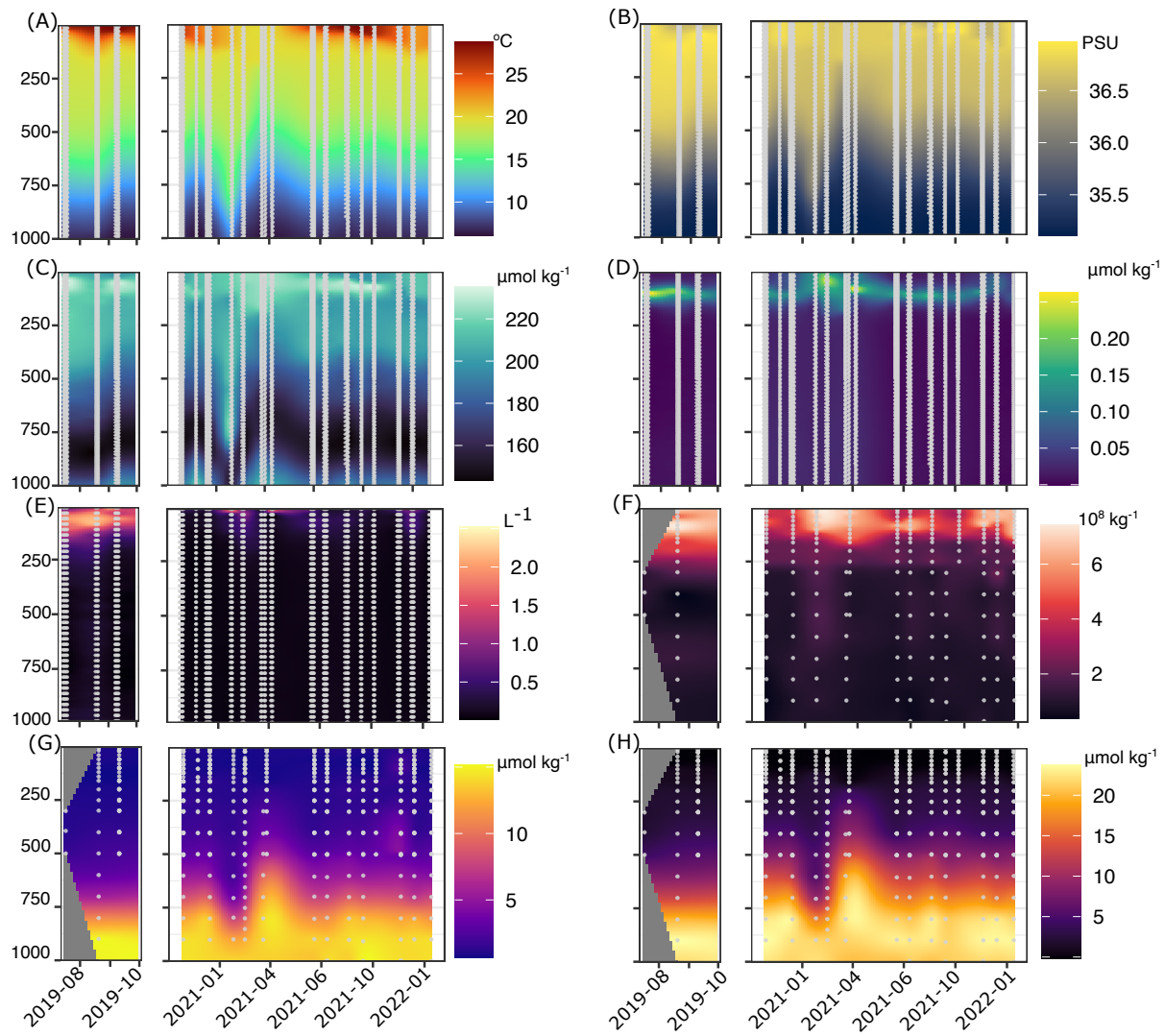


Figure 2: Environmental profiles across time-series of study period. Y axis shows depth in meters. (A) Temperature. (B) Salinity. (C) Dissolved Oxygen. (D) in situ chlorophyll fluorescence. (E) Particle concentration ($184 - 900 \mu\text{m m}^3$). (F) Bacteria Abundance. (G) Silica. (H) Nitrate

198 Overall, particle concentration was high near the surface during the 2021 spring bloom, then moved deeper
 199 throughout the water column attenuating throughout the lower epipelagic (Figure 2E). Similarly, het-
 200 erotrophic bacteria abundance was closely linked to overall productivity, although there was a more con-

201 sistent moderate-abundance layer near the top of the mesopelagic (~250m) (Figure 2F). Concurrent with
202 the secondary fall production peak, there was also higher particle concentration and bacterial abundance in
203 the later summer and early fall. Interestingly, while primary productivity estimates from July-August were
204 not that different between 2019 and 2021 (Figure 3A), chlorophyll-a florescence, particle concentration, and
205 bacterial abundance were much higher in 2019's summer/fall (Figure 2D-F). Inorganic nutrients (*Si* and
206 NO_3) were generally well stratified, with low concentrations in the epipelagic and increasing throughout the
207 mesopelagic. However, both nutrients did vary vertically in accordance with the 2021 February downwelling
208 and spring mixing period (Figure 2G-H). Additionally, in the late fall of 2021, *Si* concentrations were slightly
209 elevated in the mid-mesopelagic (Figure 2G).

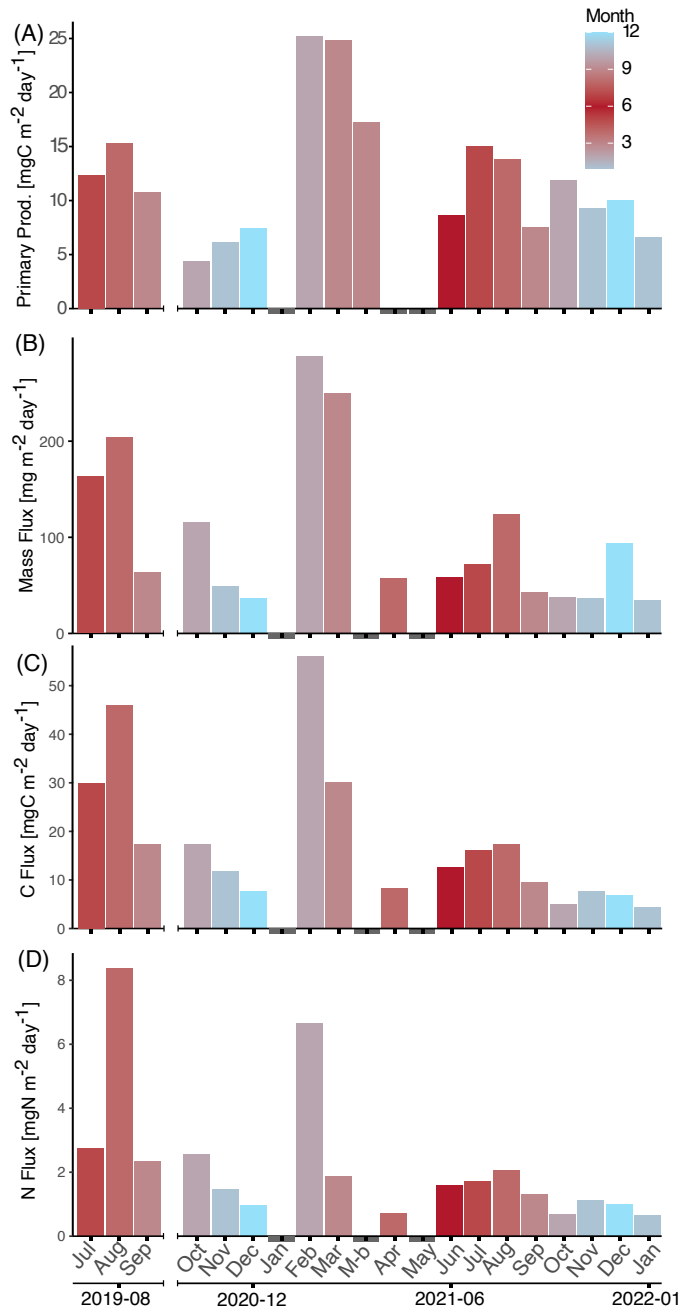


Figure 3: Primary productivity (A) and flux estimates from total mass (B), carbon (C), and nitrogen (D). Values are from monthly cruises with month displayed in corresponding colors. Absent data are shown by grey bar.

210 Overall mass flux to the mesopelagic was highest during the 2021 February downwelling (Figure 3B). Gen-
211 erally, export was similarly high during March, declining in April then increasing slightly throughout the
212 summer and early fall. While magnitude was slightly different, this pattern was consistent with total mass,
213 carbon and nitrogen fluxes (Figure 3B-D). Higher mass, carbon and nitrogen flux also occurred in the 2019
214 late summer - early fall period.

215 **Rhizaria abundance and distribution**

216 Across all imaged mesozooplankton ($>900\mu m$), Rhizaria comprised a considerable fraction of the total com-
217 munity. Considering the total abundances of the observational period, Rhizaria comprised on average, 42.6%
218 of all mesozooplankton abundance (Supplemental Figure 3). Copepods were the second most abundant, com-
219 prising 35.5% and all other living mesozooplankton were 22%. The large contribution of Rhizaria to the
220 mesozooplankton community is most prominent in the epipelagic, where they accounted for 47% of all meso-
221 zooplankton abundance. In the mesopelagic Rhizaria were a smaller fraction, at 38% in the upper layers
222 (200-500m) and 37% in the deeper mesopelagic (500-1000m).

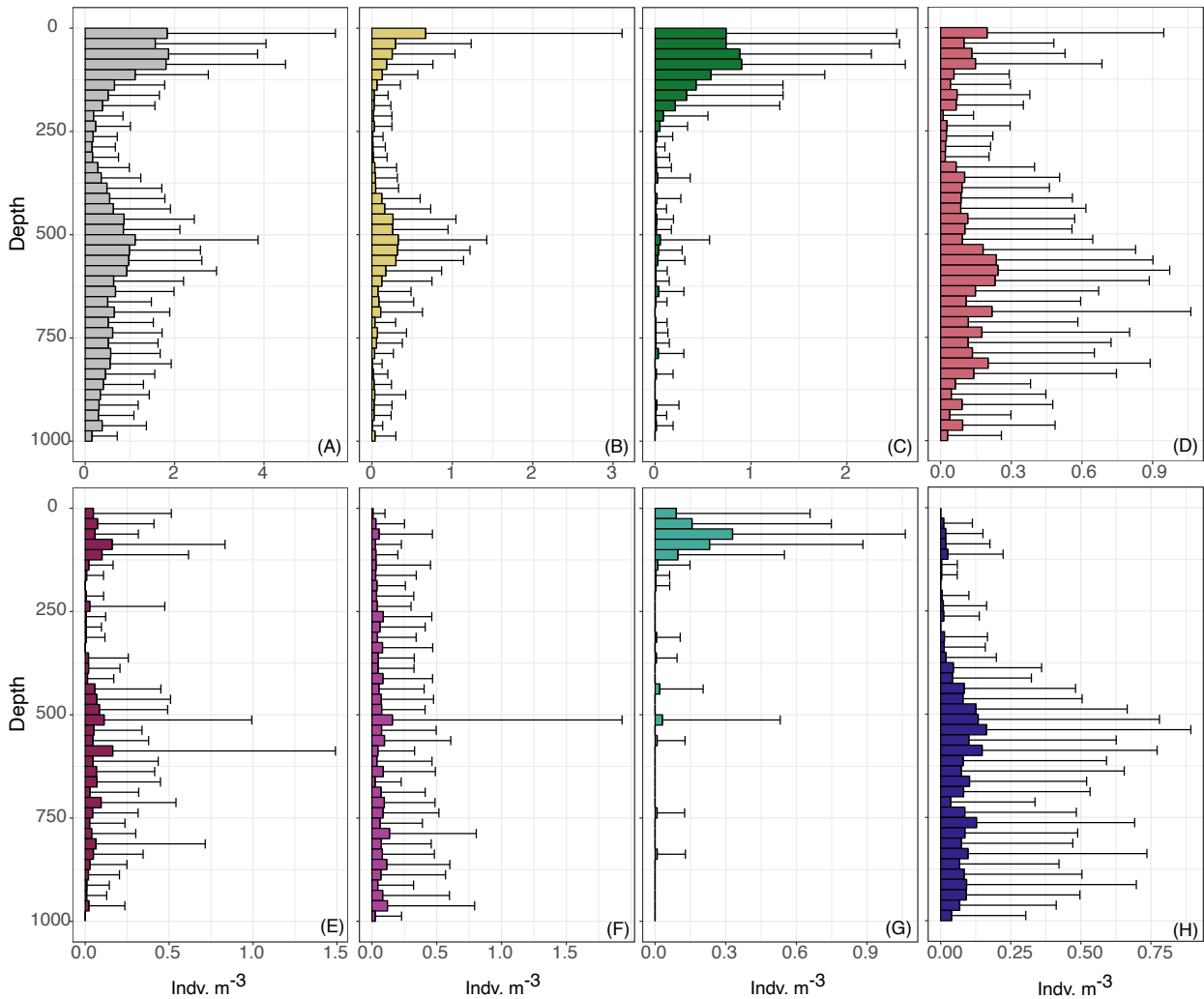


Figure 4: Average abundance of Rhizaria in 25m bins, across entire study period. Shown are total Rhizaria (A), Acantharea (B), Collodaria (C), Aulacanthidae (D), Foraminifera (E), Aulosphaeridae (F), Castanellidae (G), Coelodendridae (H).

223 Average abundance of all Rhizaria had a bimodal distribution with respect to depth. Total abundance was
 224 highest just below the surface (0-100m), with secondary, wider peak occurring in the mid mesopelagic (Fig-
 225 ure 4A). Variation in depth binned abundance was large, likely due to seasonal variability but also increased
 226 from the detection-risk described in the methods. The vertical distribution pattern and abundance varied

227 considerably across taxonomic groups. Radiolaria were some of the most abundant taxa observed, particu-
228 larly in the epipelagic (Figure 4, Figure 5A). Acantharea displayed a bimodal distribution accounting for a
229 large portion of the total Rhizaria pattern (Figure 4B, Figure 5). The surface layers were largely comprised of
230 Collodaria, whose colonies were abundant (Figure 4C). The most abundant Phaeodaria, Aulacanthidae, also
231 had a bimodal pattern with the density was highest in the lower mesopelagic (Figure 4D). Foraminifera had a
232 similar bimodal distribution, yet their overall average densities were much lower (Figure 4E). Aulosphaeridae
233 had low average density and was nearly homogeneously distributed throughout the water column, although
234 slightly lower in the epipelagic (Figure 4F). Castanellidae were the only Phaeodaria who appeared to be
235 effectively restricted to the photic zone (Figure 4G). Alternatively, Coelodendridae primarily occurred in
236 the lower mesopelagic (Figure 4H). A few individuals from the families Tuscaroridae and Medusettidae were
237 also observed in the mesopelagic, yet they were much rarer (data not shown).

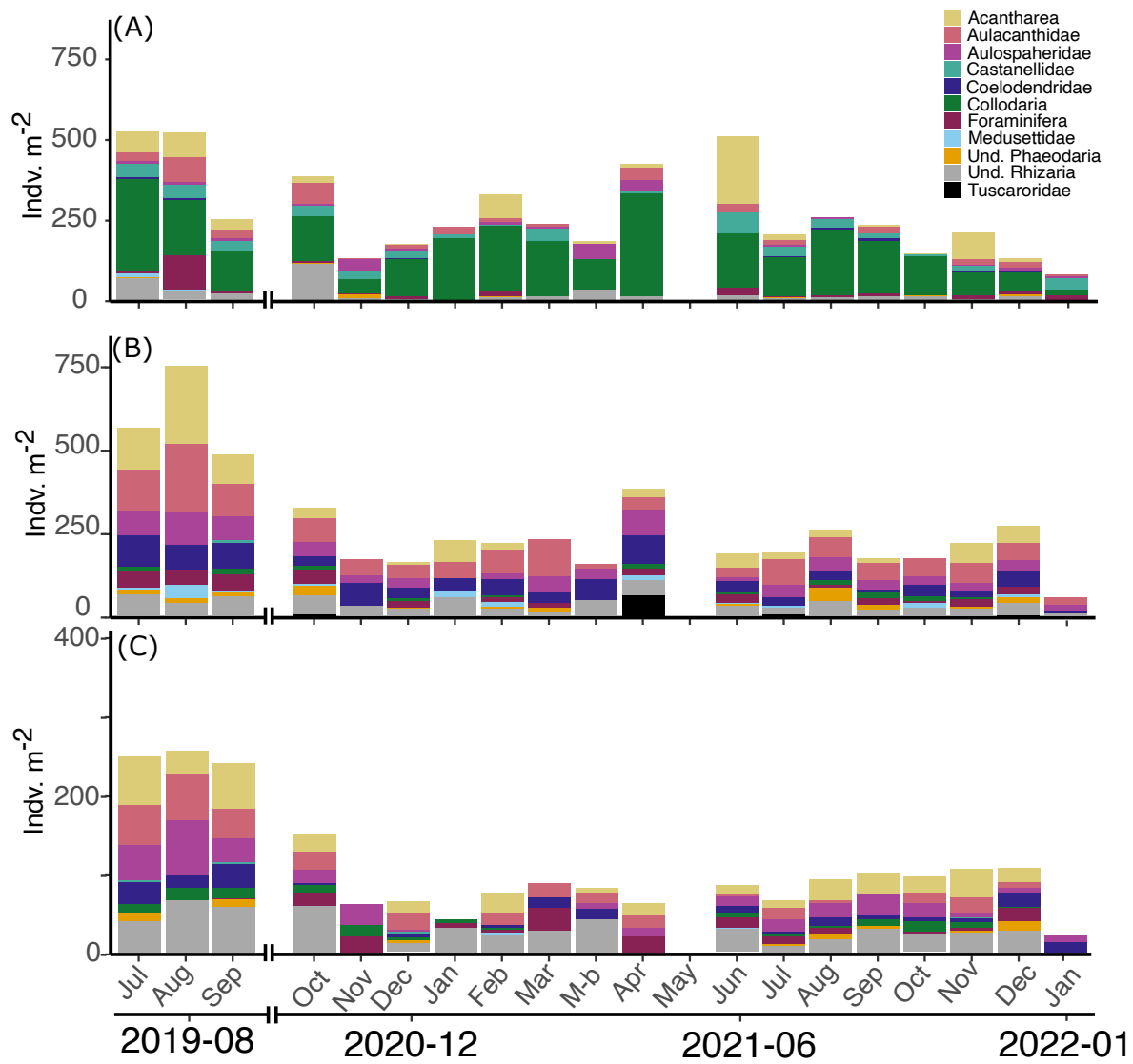


Figure 5: Seasonality of Rhizaria integrated abundance for the epipelagic (0-200m) (A), upper mesopelagic (200-500m) (B), lower mesopelagic (500-1000m) (C). Data shown are the cruise mean integrated abundance in the water column region colored for each taxon.

238 Between the monthly cruises, Rhizaria integrated abundance varied in the epipelagic. Highest average abun-
 239 dance occurred in June 2021 and was lowest during the winter months (Figure 5A). The 2019 later summer

²⁴⁰ - fall period also had much higher integrated abundance than similar months in 2021. While the majority
²⁴¹ of integrated abundance in the epipelagic was consistently attributable to Collodaria, Acanthrea abundance
²⁴² occurred sporadically and could account for a large portion of the total in some months (Figure 5A). The
²⁴³ mesopelagic integrated abundance was much more consistent across monthly cruises, although average abun-
²⁴⁴ dance was notably higher in 2019 (Figure 5B, 5C). The community composition in the mesopelagic was more
²⁴⁵ diverse, mostly comprised of Phaeodaria families. However, Acantharea and unidentified Rhizaria also were
²⁴⁶ common members of the community (Figure 5B, C).

²⁴⁷ **Body size throughout the water column.**

²⁴⁸ Very few taxa had consistent distributions throughout the water column. Only Acanthrea, Foraminifera,
²⁴⁹ Aulacanthidae, and Aulosphaeridae were consistently abundant in the epipelagic and mesopelagic. To inves-
²⁵⁰ tigate if the populations or morphologies shifted throughout the water column, we compared the sizes (ESD)
²⁵¹ between mesopelagic and epipelagic groups for each taxa. All groups were significantly different on average
²⁵² (Wilcox Rank Sum p-value <0.001). Acantharea were smaller, on average in the mesopelagic while all other
²⁵³ taxa tended to be larger (Figure 6).

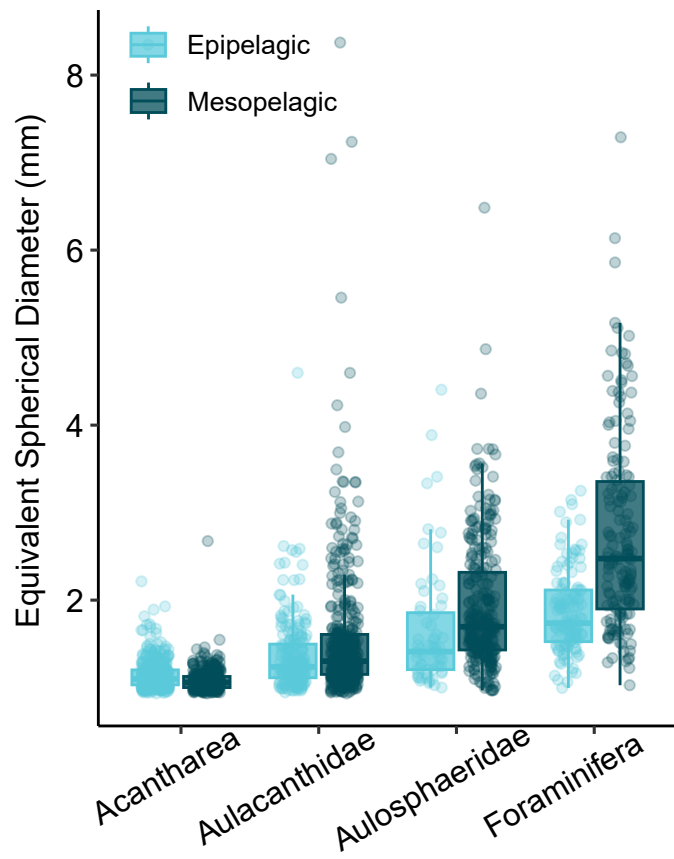


Figure 6: Comparison of average sizes (ESD) amongst Rhizaria taxa which occurred throughout the water column.

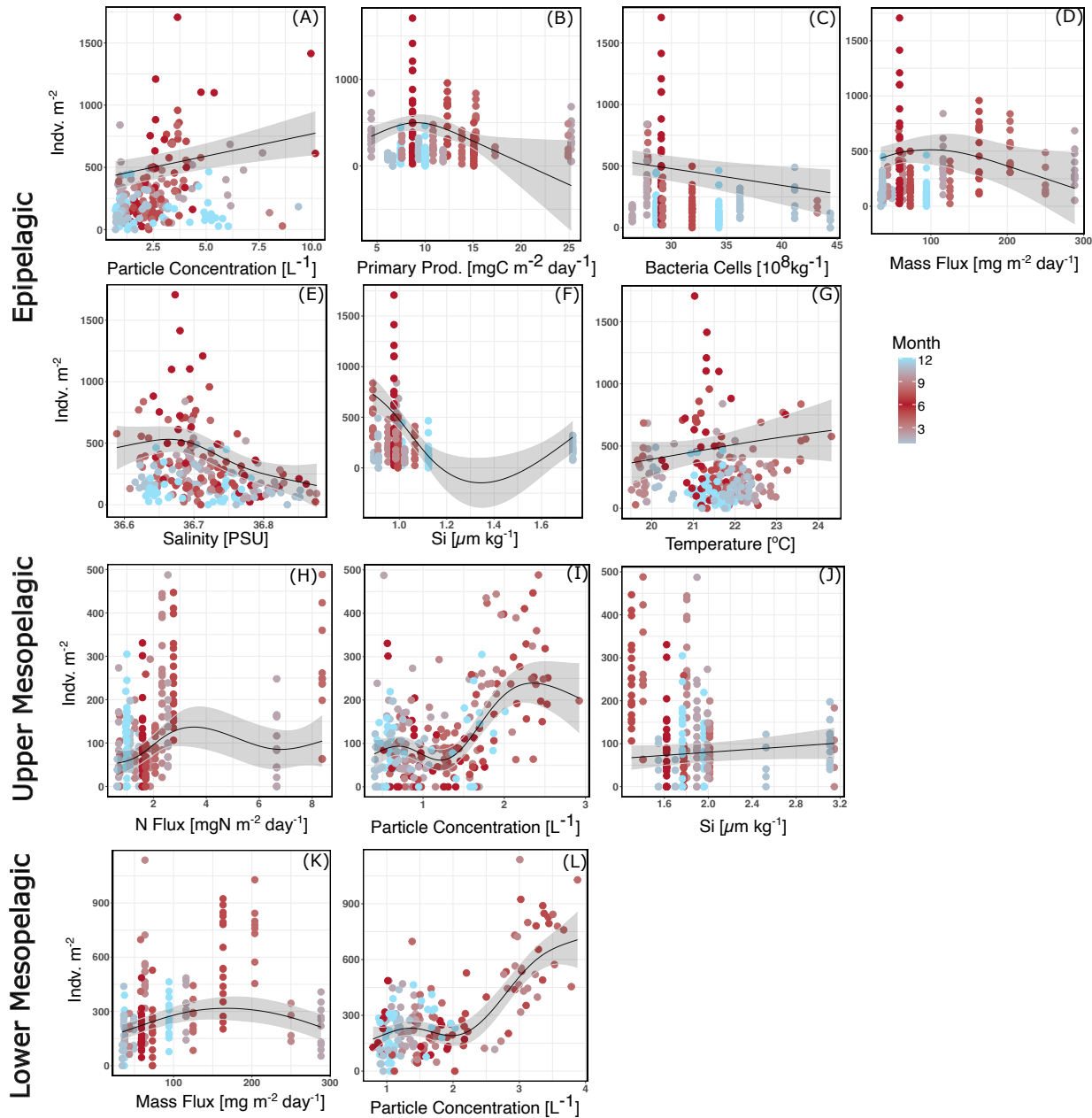


Figure 7: Partial effect plots from Generalized Additive Models (GAMs) of all Rhizaria abundance. Models were constructed separately for depth integrated abundance through the Epipelagic (0-200m) (A-G), Upper Mesopelagic (200-500m) (H-J), and the Lower Mesopelagic (500-1000m) (K-L). Each panel represents the partial effect of a GAM model term, with smoothed relationship shown shaded with 95% confidence intervals. Individual points are depth integrated values for all Rhizaria from an individual cast, colored by month.

255 For integrated abundance of all Rhizaria, the GAMs produced moderate fits ($R^2_{adj} = 0.406\text{-}0.603$) (Table
 256 1). In the epipelagic, there were several significant predictor variables (Figure 7A-7G). This included terms
 257 which are likely indicators of changing water masses; Salinity (7E) and Temperature (7G). The model
 258 also had parameters related to both heterotrophy (Particle concentration, 7A) and autotrophy (Primary
 259 production, 7B). However the relationship to particle concentration is weakly increasing trend while the
 260 primary productivity effect appears to be influenced by a cruise with a high outlier for increased primary
 261 productivity. The models for the mesopelagic regions were much more reduced and the only significant
 262 effects were particle-related terms (particle concentration and mass flux). In the upper mesopelagic (Figure
 263 7H-7J), final model included N flux, particle concentration and a non-significant effect for Silica. The lower
 264 mesopelagic (Figure 7K, 7L) only had model effects kept of total mass flux and particle concentration. For
 265 both the upper and lower mesopelagic, particle concentration had a clear, strong positive relationship (Figure
 266 7I, 7L).

Table 1: Generalized Additive Model results for integrated total Rhizaria abundance in different regions of the water column. edf = estimated degrees of freedom, F = F-statistic, p = p-value. Models were selected using a backwards-stepwise approach with a retention threshold of $p = 0.1$ or a large enough reduction in model fit.

Model	Term	edf	F	p
All Rhizaria Epipelagic	Temperature	0.7950	0.492	0.0440
$R^2_{adj} = 0.48$	Salinity	2.4117	5.113	<0.001
	Silica	2.1511	8.601	<0.001
	Bacteria Concentration	0.8870	1.544	<0.001
	Avg Mass Flux	1.4107	0.802	0.0211
	Primary Productivity	1.9280	2.736	<0.001
	Particle Concentration	0.9151	2.136	<0.001

Model	Term	edf	F	p
All Rhizaria Upper Mesopelagic	Silica	0.6702	0.404	0.0814
$R^2_{adj} = 0.40$	Avg N Flux	2.9524	3.172	<0.001
	Particle Concentration	3.5568	11.82	<0.001
All Rhizaria Lower Mesopelagic	Avg Mass Flux	2.036	2.953	<0.001
$R^2_{adj} = 0.61$	Particle Concentration	3.819	27.43	<0.001

267 GAMs for individual taxa were much less consistent in their fits (Table 2). This is likely in part due to
 268 the high number of non-observations for certain taxa. Note that due to low abundances, GAMs were not
 269 constructed for Tuscaroridae or Medusettidae. Furthermore no, significant terms were found for a model
 270 with Aulosphaeridae in the epipelagic nor Foraminifera in the mesopelagic.

271 Epipelagic Acantharea were explained by several predictor variables and had a good fit ($R^2_{adj} = 0.539$,
 272 Table 2, Supplemental FIgure 4). Foraminifera had a good fitting GAM in the epipelagic ($R^2_{adj} = 0.543$).
 273 There were several significant explanatory variables, although the clearest pattern was observed of high
 274 temperatures associated with more Foraminifera abundance (Table 2, Supplemental Figure 4U). Epipelagic
 275 Aulacanthidae similarly had several predictor variables which were significant, including both water quality
 276 parameters and particle/flux predictors (Table 2). There was a weak fit for Collodaria in the epipelagic
 277 ($R^2_{adj} = 0.16$), although there was a logit-like relationship where higher abundances tended to occur during
 278 higher DO conditions in the surface waters (Supplemental Figure 4). Castanellidae also had a weak model
 279 fit in the epipelagic ($R^2_{adj} = 0.228$), although particle concentration was the strongest predictor term (Table
 280 2, Supplemental Figure 4).

Table 2: Taxa-specific generalized additive models for different regions of the water column.edf = estimated degrees of freedom, F = F-statistic, p = p-value. Models were selected using a backwards-stepwise approach with a retention threshold of p = 0.1 or a large enough reduction in model fit.

Model	Term	edf	F	p
Acantharea Epipelagic	Temperature	0.868	0.380	0.0935
$R^2_{adj}=0.539$	Salinity	2.349	4.646	<0.001
	O2	2.501	5.493	<0.001
	Avg Mass Flux	4.815	22.59	<0.001
	Bacteria	1.608	1.360	0.00945
	Particle Concentration	0.877	1.414	0.00449
Acantharea Upper Mesopelagic	Avg Mass Flux	1.866	1.220	0.0166
$R^2_{adj}=0.197$	Avg N Flux	2.208	3.100	<0.001
	Primary Productivity	2.382	2.497	<0.001
	Particle Concentration	0.724	0.521	0.0437
Acantharea Lower Mesopelagic	Temperature	1.958	2.986	<0.001
$R^2_{adj}=0.496$	Avg N Flux	1.513	1.565	0.0037
	Primary Productivity	0.856	1.153	0.0045
	Particle Concentration	1.661	8.667	<0.001
Aulacanthidae Epipelagic	Temperature	2.591	5.003	<0.001
$R^2_{adj}=0.394$	Salinity	1.523	1.789	0.002
	RFU	0.872	1.315	0.0042
	Bacteria	0.808	0.833	0.0160
	Primary Productivity	2.622	9.160	<0.001

Model	Term	edf	F	p
	Particle Concentration	1.937	2.751	<0.001
Aulacanthidae Upper Mesopelagic	Avg C Flux	1.675	1.408	0.0109
$R_{adj}^2=0.132$	Particle Concentration	2.308	2.476	0.0013
Aulacanthidae Lower Mesopelagic	Avg Mass Flux	1.476	1.418	0.0076
$R_{adj}^2=0.308$	Particle Concentration	2.457	7.756	<0.001
Aulosphaeridae Upper Mesopelagic	Particle Concentration	2.778	12.76	<0.001
$R_{adj}^2=0.196$				
Aulosphaeridae Lower Mesopelagic	Particle Concentration	2.012	6.306	<0.001
$R_{adj}^2=0.148$				
Castanellidae Epipelagic	Salinity	0.915	0.400	0.0935
$R_{adj}^2=0.228$	RFU	0.912	2.052	<0.001
	Si	2.018	3.656	<0.001
	Bacteria	1.128	0.883	0.0170
	Particle Concentration	2.278	4.028	<0.001
Coelodendridae Upper Mesopelagic	Avg N Flux	0.734	0.551	0.0527
$R_{adj}^2=0.09$	Particle Concentration	0.965	5.102	<0.001
Coelodendridae Lower Mesopelagic	Particle Concentration	3.051	6.768	<0.001
$R_{adj}^2=0.157$				
Collodaria Epipelagic	Salinity	0.926	2.267	<0.001
$R_{adj}^2=0.16$	O2	2.015	2.217	<0.001
	Bacteria	1.843	2.100	0.0024
Foraminifera Epipelagic	Temperature	4.420	7.624	<0.001

Model	Term	edf	F	p
$R^2_{adj}=0.543$	O2	0.799	0.788	0.023
	Bacteria	0.000	0.000	0.523
	Avg N Flux	1.847	3.022	<0.001
	Primary Productivity	0.472	0.139	0.183
	Particle Concentration	1.685	2.955	<0.001

281 In the upper mesopelagic (200-500m), abundances were generally low (Figure 4) so GAMs were only con-
 282 structed for Acantharea, Aulacanthidae, Aulosphaeridae, and Coelodendridae (Table 2). All these models
 283 had generally poor fits ($R^2_{adj} < 0.20$). Yet, for all upper mesopelagic models, particle concentration was a
 284 significant explanatory variable (Table 2, Supplemental Figure 5). The lower mesopelagic also had generally
 285 poor GAM fits for taxon specific models ($R^2_{adj} < 0.31$), with the exception of Acantharea ($R^2_{adj} = 0.496$).
 286 Acantharea in the lower mesopelagic was most clearly positively associated with particle concentration (Sup-
 287 plemental Figure 6). For all Phaeodaria with a significant model, particle concentration was a main predictor
 288 variable (Table 2, Supplemental Figure 6).

289 Discussion

290 Overall Rhizaria abundance and patterns

291 In the epipelagic Rhizaria exhibited a notable seasonal pattern. Rhizaria abundances were higher in the
 292 summer months and lower during the winter. During a prior time period, Blanco-Bercial *et al.* (2022) noted
 293 that there is considerable seasonality in the community composition of all protists. Despite the seasonality
 294 of Rhizaria abundance, community composition was relatively consistent, with Collodaria representing the

295 bulk of the community. It should be noted that the overall taxonomic resolution of the UVP5 is fairly
296 low, so there may be a switching of species within the broad groups identified in this study which were not
297 captured. Throughout the mesopelagic, month-to-month variation in 2021 was relatively low. Again, this is
298 consistent with observations from metabarcoding of the whole protist community in the same study region
299 (Blanco-Bercial *et al.*, 2022). This finding is not surprising as the overall seasonal variation in environmental
300 conditions in this region were low.

301 Overall Rhizaria were the most commonly identified group of mesoplankton throughout the study period.
302 We do note that the UVP5 commonly captures *Trichodesmium* colonies, yet these were excluded in this
303 comparison as they are strictly autotrophs. It should be noted that previous work has suggested that
304 avoidance behavior with the UVP is possible, at times likely, for visual and highly mobile zooplankton
305 (Barth and Stone, 2022). Thus, the percent contribution reported here (42.7%) of Rhizaria to the total
306 mesozooplankton community may be inflated due to under sampling of organisms such as Euphausiids and
307 Chaetognaths which have quick escape responses. Regardless, it is worth noting that in the same region,
308 with data collected in 2012 and 2013 using similar calculation methods, Biard *et al.* (2016) estimated large
309 Rhizaria only contribute 15% of the total mesozooplankton community in the upper 500m. Likely, Rhizaria
310 display considerable interannual variability. In the present study, we noticed considerably higher Rhizaria
311 abundance throughout the water column in 2019 compared to 2021. Similarly, in the California Current a
312 multi-year study of Aulosphaeridae saw considerable variation between years (Biard *et al.*, 2018). To truly
313 understand the drivers of interannual variability however, sustained observations of Rhizaria over longer time
314 periods are required.

315 **Relationship to environmental parameters**

316 In general, the fit of most GAMs were moderate to poor. One possible reason for the poor fits may have
317 been that for some taxa, conditions were not variable enough to capture a range of conditions at which
318 they may exist. For instance, Collodaria were the most abundant taxa observed, yet the fit of their GAM
319 was particularly poor. In studies which covered a wider range of parameters, Collodaria has been shown
320 to strongly vary with changes in parameters such as temperature, chlorophyll-a, mixing, and water clarity
321 (Biard *et al.*, 2017; Biard and Ohman, 2020). Alternatively, Acantharea had relatively good fitting GAMs.
322 These taxa also had some of the largest variation from month to month on cruises. Thus, it may be that
323 in the oligotrophic, the relatively stable conditions can support certain taxa while others are more sporadic.
324 It should also be noted that due to the challenge of adequately sampling enough volume to overcome low-
325 detection issues, GAMs were run on integrated data. However, variation with environmental parameters
326 throughout the water column are likely, just not captured in the modelling aspect of this study. Future
327 studies which are able to account for detection biases in finer vertical resolution of Rhizaria may improve
328 ecological models of their abundance. One consistent parameter which had significant positive associations
329 was particle concentration. This observation is not surprising as most Rhizaria likely to some extent engage
330 in flux feeding.

331 **Vertical Structure and Trophic Roles**

332 In this study we present a clear pattern of vertical zonation between different Rhizaria groups. Largely, the
333 taxonomic composition and vertical positioning were similar to Rhizaria zonation in the California Current
334 Ecosystem (Biard and Ohman, 2020). It should be noted however, that the secondary abundance peak
335 reported in the present study is lower. This is likely due to the more oligotrophic nature of the study region,
336 where the euphotic zone penetrates deeper into the water column. Most prevalent in the epipelagic were

337 Collodaria. These mixotrophic Radiolaria have long been reported to contribute to primary productivity in
338 the euphotic zone (Michaels *et al.*, 1995; Dennett *et al.*, 2002). Collodaria are thought to be particularly
339 successful globally in oligotrophic regions due to their photosymbiotic relationships (Biard *et al.*, 2016, 2017).
340 We observed the highest abundance of Collodaria during June 2021, supporting the notion they can thrive
341 during the typically low-nutrient conditions of summer stratification. However, Collodaria also increased
342 during the spring mixing period, suggesting that they can thrive during conditions which may typically be
343 thought to favor autotrophs. Furthermore, while Collodaria were primarily absent from below 250m, there
344 were a few instances of deeper colonies being observed. Global investigations of polycystine flux, suggest
345 that deep-Collodaria in oligotrophic regions may be a consequence of isothermal submersion (Boltovskoy,
346 2017). Alternatively, surface waters at BATS often mix into the mode water during the seasonal mixing, so
347 Collodaria in the deeper waters may be a result of diapycnal mixing. Another effectively exclusively epipelagic
348 Rhizaria was the Phaeodaria family of Castanellidae. All Phaeodaria are thought to be fully heterotrophic
349 (Nakamura and Suzuki, 2015), nonetheless a number of studies, including this one, report Castanellidae to
350 be typically found in the lower epipelagic (Zasko and Rusanov, 2005; Biard *et al.*, 2018; Biard and Ohman,
351 2020). It should be considered that perhaps Castanellidae specializes in feeding on sinking particles directly
352 at the base of the epipelagic. Given it's smaller size (Nakamura and Suzuki, 2015), Castanellidae does not
353 need a large diameter to efficiently flux feed at the typically particle rich region of the lower epipelagic.
354 The mesopelagic generally was home to known heterotrophic organisms, particularly for those which were
355 constrained to exclusively occupy deeper waters. This is consistent with Blanco-Bercial *et al.* (2022)'s
356 observation of an auto-/mixotroph to heterotroph gradient in local protist community as well as global
357 patterns in Rhizaria ecology [Laget *et al.* (2024)]. The upper mesopelagic interestingly had relatively
358 low total abundance. This low-abundance region likely reflects the dynamics of productivity and export
359 throughout the water column. While productivity and thus sinking particles for flux feeders are high in the

360 euphotic zone, much of this is attenuated throughout the epipelagic. So, while the base of the epipelagic
361 may provide a rich feeding environment for Castanellidae, smaller protists, or heterotrophic bacteria (Figure
362 2F), the region from 200-500m might be otherwise food poor. Perhaps it is more advantageous for Rhizaria
363 to situate deeper, in darker regions of the twilight zone where visual predators and vertically migrating
364 organisms may not feed on them. Also it should be noted that Phaeodaria utilize silica to build their opaline
365 tests, and silica concentrations started to increase around 500m (Figure 2G). However, *Si* was not a significant
366 term for any taxon-specific model in the mesopelagic. Aulosphaeridae was only found to have significant
367 relationships, although weak fits, to particle concentration in the mesopelagic. In our study, while consistently
368 observed, overall abundances of Aulosphaeridae were very low. In the Pacific Ocean, on California's Coast,
369 much higher abundances of Aulosphaeridae have been reported [Zasko and Rusanov (2005); Biard and
370 Ohman (2020)] and they have massive potential to impact silica export (Biard *et al.*, 2018). Coelodendridae
371 were also seemingly restricted to the deeper section of the mesopelagic. This is interesting given that in the
372 California Current, (Biard and Ohman, 2020) found a bimodal distribution in Coelodendridae. There are
373 several morphotypes corresponding to different taxa of Coelodendridae (Nakamura and Suzuki, 2015; Biard
374 and Ohman, 2020). So it may be that only a few types of Coelodendridae were observed in this study, while
375 the epipelagic variety was not. Alternatively, the lower epipelagic of the extremely productive California
376 Current may provide adequate habitat for Coelodendridae, which is not available in the oligotrophic Sargasso
377 Sea.

378 A number of taxa were found to have a bimodal distribution, with sizable populations in both the epipelagic
379 and mesopelagic. Aulacanthidae had a bimodal distribution, although abundances were highest in the lower
380 mesopelagic. Foraminifera also had a bimodal distribution. Some lineages of Foraminifera are known to
381 host photosymbionts (Kimoto, 2015; Biard, 2022b), however they are also efficient predators commonly seen
382 throughout the mesopelagic (Caron and Be, 1984; Gaskell *et al.*, 2019). Thus it is not surprising to find

their presence in both locations of the water column. Foraminifera are also known to vary their vertical distribution across their life cycle in phase with lunar cycles (Bijma *et al.*, 1990; Kimoto, 2015; Gaskell *et al.*, 2019; Biard, 2022b). However, the sampling scheme of the BATS program does not capture this frequency and was not investigated in the present study.

Acantharea also had a bimodal distribution, with much more sizable abundances than Aulacanthidae or Foraminifera. Most prior studies of Acantharea vertical distribution found them concentrated in near surface layers of the water column Zasko and Rusanov (2005). This would support the paradigm that large Acantharea abundances may be supported by their mixotrophic abilities (Michaels *et al.*, 1995; Suzuki and Not, 2015). While the UVP5 images cannot distinguish between mixotrophic and heterotrophic Acantharea, the GAMs constructed for Acantharea abundance found positive associations with particle concentration and mass flux, suggesting a higher reliance on heterotrophy. Recently Mars Brisbin *et al.* (2020) described apparent predator behavior amongst near-surface Acantharea. Thus it is likely that epipelagic Acantharea may commonly be heterotrophic or mixotrophic with an increased reliance on heterotrophy. Yet, it should be noted in the Sargasso Sea, both heterotrophic and symbiotic lineages of Acantharea have been reported (Blanco-Bercial *et al.*, 2022). Additionally, Michaels (1988) noted that the majority of Acantharea (by abundance) were smaller than $160\mu m$. While that estimate may be inflated due to inability to capture larger cells, small Acantharea were not captured in the present study. Thus, trophic strategy may shift based on sizes of Acantharea.

Decelle *et al.* (2013) proposed a hypothetical life cycle for cyst-bearing (strictly heterotrophic) Acantharea. This hypothesized life cycle suggests that epipelagic Acantharea are adult populations, which form cysts that sink into the mesopelagic, then reproduce and rise. Furthermore, given that horizontal transfer of symbionts between generations of Acantharea is unlikely due to their spawning behavior, the newly spawned mesopelagic Acantharea are not necessarily required to rapidly return to the photic zone (Decelle *et al.*,

406 2012, 2013). This hypothesis predicts that Acanthareas in the mesopelagic would be smaller (Decelle *et al.*,
407 2013). Mars Brisbin *et al.* (2020) provided some support for this hypothesis, with a significant decrease
408 in Acantharea sizes with depth. Although the authors also observed low abundances in the mesopelagic
409 and noted that the smaller sizes may be due to lower food availability (Mars Brisbin *et al.*, 2020). Since
410 food is more scarce in the mesopelagic, nutritional quality lower, yet flux feeders would likely grow larger
411 to increase their feeding range (Stukel *et al.*, 2018; Biard and Ohman, 2020). In the data collecting in
412 this study, Acanthareas in the mesopelagic were significantly smaller than the epipelagic, despite the other
413 bimodal taxa (Foraminifera and Aulacanthidae) being significantly larger with depth. This provides added
414 support for the hypothesis that cyst-forming Acantharea may utilize different sections of the water column
415 throughout their life cycle. However to further investigate this, more work is needed with higher temporal
416 and taxonomic resolution.

417 **Conclusions and Considerations**

418 This study provides a detailed look at Rhizaria abundance over time throughout the water column in a
419 major oligotrophic gyre. We show that their abundances are generally related to particle concentration and
420 flux, although lack of environmental variability may have reduced the fit of our GAMs. Considering the
421 potential role of Rhizaria in the biological carbon pump, they may have a somewhat mixed role. In the
422 shallower regions, they may be an attenuating force on sinking particles (Stukel *et al.*, 2019). However,
423 once consumed and repackaged by larger Rhizaria, they can sink quicker and contribute more to overall flux
424 (Michaels, 1988). Thus, Rhizaria may act as an aggregation mechanism. However, to truly test this, more
425 work is needed measuring Rhizaria flux.

426 The vertical partitioning documented in this study do support the hypothesis that mixotrophic rhizaria will
427 occupy shallower waters while deeper waters are dominated by heterotrophy. However the degree to which

428 mixotrophic Rhizaria in the euphotic zone rely on heterotrophy versus symbiosis is uncertain. Collodaria
429 were recorded as consistent and dominant members of the near surface region. These organisms have the
430 potential to contribute considerably to the otherwise low productivity of oligotrophic regions. However, their
431 role in food webs is not well understood. While this study represents a step-forward in our understanding
432 of Rhizaria ecology, continued research on Rhizaria is much needed to better understand their ecology.
433 Particularly extended work describing interannual patterns in Rhizaria abundance. Also work defining
434 biotic interactions, feeding rates, productivity, and life history are all rich fields of interest in Rhizaria.

435 **References:**

- 436 Anderson, O. R. (2014) Living Together in the Plankton: A Survey of Marine Protist Symbioses. *Acta*
437 *Protozoologica*, **53**, 29–38.
- 438 Anderson, O. R. and Bé, A. W. H. (1976) A CYTOCHEMICAL FINE STRUCTURE STUDY OF
439 PHAGOTROPHY IN A PLANKTONIC FORAMINIFER, *HASTIGERINA PELAGICA* (d'ORBIGNY).
440 *The Biological Bulletin*, **151**, 437–449.
- 441 Barth, A. and Stone, J. (2022) Comparison of an in situ imaging device and net-based method to study
442 mesozooplankton communities in an oligotrophic system. *Frontiers in Marine Science*, **9**.
- 443 Barth, A. and Stone, J. (2024) Understanding the picture: The promises and challenges of in-situ imagery
444 data in the study of plankton ecology. *Journal of Plankton Research: Horizons*, 1–15.
- 445 Benfield, M. C., Davis, C. S., Wiebe, P. H., Gallager, S. M., Gregory Lough, R., and Copley, N. J. (1996)
446 Video Plankton Recorder estimates of copepod, pteropod and larvacean distributions from a stratified
447 region of Georges Bank with comparative measurements from a MOCNESS sampler. *Deep Sea Research*
448 *Part II: Topical Studies in Oceanography*, **43**, 1925–1945.
- 449 Biard, T. (2022a) Diversity and ecology of Radiolaria in modern oceans. *Environmental Microbiology*, **24**,

- 450 2179–2200.
- 451 Biard, T. (2022b) *Rhizaria*. Encyclopeida of Life Sciences, pp. 1–11.
- 452 Biard, T., Bigeard, E., Audic, S., Poulain, J., Gutierrez-Rodriguez, A., Pesant, S., Stemmann, L., and Not,
453 F. (2017) Biogeography and diversity of Collodaria (Radiolaria) in the global ocean. *The ISME Journal*,
454 **11**, 1331–1344.
- 455 Biard, T., Krause, J. W., Stukel, M. R., and Ohman, M. D. (2018) The Significance of Giant Phaeodarians
456 (Rhizaria) to Biogenic Silica Export in the California Current Ecosystem. *Global Biogeochemical Cycles*,
457 **32**, 987–1004.
- 458 Biard, T. and Ohman, M. D. (2020) Vertical niche definition of test-bearing protists (Rhizaria) into the
459 twilight zone revealed by in situ imaging. *Limnology and Oceanography*, **65**, 2583–2602.
- 460 Biard, T., Stemmann, L., Picheral, M., Mayot, N., Vandromme, P., Hauss, H., Gorsky, G., Guidi, L., et al.
461 (2016) In situ imaging reveals the biomass of giant protists in the global ocean. *Nature*, **532**, 504–507.
- 462 Bijma, J., Erez, J., and Hemleben, C. (1990) Lunar and semi-lunar reproductive cycles in some spinose
463 planktonic foraminifers. *Journal of Foraminiferal Research*, **20**, 117–127.
- 464 Blanco-Bercial, L. (2020) Metabarcoding analyses and seasonality of the zooplankton community at BATS.
465 *Frontiers in Marine Science*, **7**.
- 466 Blanco-Bercial, L., Parsons, R., Bolaños, L. M., Johnson, R., Giovannoni, S. J., and Curry, R. (2022) The
467 protist community traces seasonality and mesoscale hydrographic features in the oligotrophic sargasso
468 sea. *Frontiers in Marine Science*, **9**.
- 469 Boltovskoy, D. (2017) Vertical distribution patterns of radiolaria polycystina (protista) in the world ocean:
470 Living ranges, isothermal submersion and settling shells. *Journal of Plankton Research*, **39**, 330–349.
- 471 Boltovskoy, D., Alder, V. A., and Abelmann, A. (1993) Annual flux of radiolaria and other shelled plankters
472 in the eastern equatorial atlantic at 853 m: seasonal variations and polycystine species-specific responses.

- 473 Deep Sea Research Part I: Oceanographic Research Papers, **40**, 1863–1895.
- 474 Caron, D. A. (2016) The rise of rhizaria | nature. *Nature*, **532**, 444–445.
- 475 Caron, D. A. and Be, A. W. H. (1984) PREDICTED AND OBSERVED FEEDING RATES OF THE
476 SPINOSE PLANKTONIC FORAMINIFER. *BULLETIN OF MARINE SCIENCE*, **35**.
- 477 Caron, D. A., Michaels, A. F., Swanberg, N. R., and Howse, F. A. (1995) Primary productivity by symbiont-
478 bearing planktonic sarcodines (acantharia, radiolaria, foraminifera) in surface waters near bermuda. *Jour-
479 nal of Plankton Research*, **17**, 103–129.
- 480 Cohen, N. R., Krinos, A. I., Kell, R. M., Chmiel, R. J., Moran, D. M., McIlvin, M. R., Lopez, P. Z., Barth,
481 A., et al. (2023) Microeukaryote metabolism across the western North Atlantic Ocean revealed through
482 autonomous underwater profiling.
- 483 Decelle, J., Colin, S., and Foster, R. A. (2015) Photosymbiosis in Marine Planktonic Protists. In Ohtsuka,
484 S., Suzaki, T., Horiguchi, T., Suzuki, N., and Not, F. (eds). Springer Japan, Tokyo, pp. 465–500.
- 485 Decelle, J., Martin, P., Paborstava, K., Pond, D. W., Tarling, G., Mahé, F., De Vargas, C., Lampitt, R.,
486 et al. (2013) Diversity, Ecology and Biogeochemistry of Cyst-Forming Acantharia (Radiolaria) in the
487 Oceans. *PLoS ONE*, **8**, e53598.
- 488 Decelle, J., Siano, R., Probert, I., Poirier, C., and Not, F. (2012) Multiple microalgal partners in symbiosis
489 with the acantharian *Acanthochiasma* sp. (Radiolaria). *Symbiosis*, **58**, 233–244.
- 490 Dennett, M. R., Caron, D. A., Michaels, A. F., Gallager, S. M., and Davis, C. S. (2002) Video plankton
491 recorder reveals high abundances of colonial radiolaria in surface waters of the central north pacific.
492 *Journal of Plankton Research*, **24**, 797–805.
- 493 Drago, L., Panaïotis, T., Irisson, J.-O., Babin, M., Biard, T., Carlotti, F., Coppola, L., Guidi, L., et al.
494 (2022) Global Distribution of Zooplankton Biomass Estimated by In Situ Imaging and Machine Learning.
495 *Frontiers in Marine Science*, **9**.

- 496 Gaskell, D. E., Ohman, M. D., and Hull, P. M. (2019) Zooglider-based measurements of planktonic
497 foraminifera in the California current system. *Journal of Foraminiferal Research*, **49**, 390–404.
- 498 Gorsky, G., Ohman, M. D., Picheral, M., Gasparini, S., Stemmann, L., Romagnan, J.-B., Cawood, A., Pesant,
499 S., et al. (2010) Digital zooplankton image analysis using the ZooScan integrated system. *Journal of*
500 *Plankton Research*, **32**, 285–303.
- 501 Gowing, M. M. (1989) Abundance and feeding ecology of Antarctic phaeodarian radiolarians. *Marine Biology*,
502 **103**, 107–118.
- 503 Gutierrez-Rodriguez, A., Stukel, M. R., Lopes dos Santos, A., Biard, T., Scharek, R., Vaulot, D., Landry,
504 M. R., and Not, F. (2019) High contribution of Rhizaria (Radiolaria) to vertical export in the California
505 Current Ecosystem revealed by DNA metabarcoding. *The ISME Journal*, **13**, 964–976.
- 506 Gutiérrez-Rodríguez, A., Lopes dos Santos, A., Safi, K., Probert, I., Not, F., Fernández, D., Gourvil, P.,
507 Bilewitch, J., et al. (2022) Planktonic protist diversity across contrasting subtropical and subantarctic
508 waters of the southwest Pacific. *Progress in Oceanography*, **206**, 102809.
- 509 Haekel, E. (1887) Report on the radiolaria collected by h.m.s. *Challenger* during the years 1873–1876, plates,
510 by ernst haekel.
- 511 Hull, P. M., Osborn, K. J., Norris, R. D., and Robison, B. H. (2011) Seasonality and depth distribution of
512 a mesopelagic foraminifer, *Hastigerinella digitata*, in Monterey Bay, California. *Limnology and Oceanog-*
513 *rphy*, **56**, 562–576.
- 514 Ikenoue, T., Kimoto, K., Okazaki, Y., Sato, M., Honda, M. C., Takahashi, K., Harada, N., and Fujiki, T.
515 (2019) Phaeodaria: An Important Carrier of Particulate Organic Carbon in the Mesopelagic Twilight
516 Zone of the North Pacific Ocean. *Global Biogeochemical Cycles*, **33**, 1146–1160.
- 517 Kimoto, K. (2015) Planktic foraminifera. pp. 129–178.
- 518 Knap, A. H., Michaels, A. F., Steinberg, D. K., Bahr, F., Bates, N. R., Bell, S., Countway, P., Close, A. R.,

- 519 *et al.* (1997) BATS methods manual, version 4.
- 520 Laget, M., Drago, L., Panaïotis, T., Kiko, R., Stemmann, L., Rogge, A., Llopis-Monferrer, N., Leynaert, A.,
- 521 *et al.* (2024) Global census of the significance of giant mesopelagic protists to the marine carbon and
- 522 silicon cycles. *Nature Communications*, **15**, 3341.
- 523 Lee, J. J. (2006) Algal symbiosis in larger foraminifera. *Symbiosis*, **42**, 63–75.
- 524 Llopis Monferrer, N., Biard, T., Sandin, M. M., Lombard, F., Picheral, M., Elineau, A., Guidi, L., Ley-
- 525 naert, A., *et al.* (2022) Siliceous rhizaria abundances and diversity in the mediterranean sea assessed by
- 526 combined imaging and metabarcoding approaches. *Frontiers in Marine Science*, **9**.
- 527 Lomas, M. W., Bates, N. R., Johnson, R. J., Knap, A. H., Steinberg, D. K., and Carlson, C. A. (2013) Two
- 528 decades and counting: 24-years of sustained open ocean biogeochemical measurements in the Sargasso
- 529 Sea. *Deep Sea Research Part II: Topical Studies in Oceanography*, **93**, 16–32.
- 530 Lombard, F., Boss, E., Waite, A. M., Vogt, M., Uitz, J., Stemmann, L., Sosik, H. M., Schulz, J., *et al.* (2019)
- 531 Globally consistent quantitative observations of planktonic ecosystems. *Frontiers in Marine Science*, **6**.
- 532 Marra, G. and Wood, S. N. (2011) Practical variable selection for generalized additive models. *Computational*
- 533 *Statistics & Data Analysis*, **55**, 2372–2387.
- 534 Mars Brisbin, M., Brunner, O. D., Grossmann, M. M., and Mitarai, S. (2020) Paired high-throughput, in
- 535 situ imaging and high-throughput sequencing illuminate acantharian abundance and vertical distribution.
- 536 *Limnology and Oceanography*, **65**, 2953–2965.
- 537 McGillicuddy, D. J., Robinson, A. R., Siegel, D. A., Jannasch, H. W., Johnson, R., Dickey, T. D., McNeil,
- 538 J., Michaels, A. F., *et al.* (1998) Influence of mesoscale eddies on new production in the Sargasso Sea.
- 539 *Nature*, **394**, 263–266.
- 540 Michaels, A. F. (1988) Vertical distribution and abundance of Acantharia and their symbionts. *Marine*
- 541 *Biology*, **97**, 559–569.

- 542 Michaels, A. F., Caron, D. A., Swanberg, N. R., Howse, F. A., and Michaels, C. M. (1995) Planktonic
543 sarcodines (Acantharia, Radiolaria, Foraminifera) in surface waters near Bermuda: abundance, biomass
544 and vertical flux. *Journal of Plankton Research*, **17**, 131–163.
- 545 Michaels, A. F. and Knap, A. H. (1996) Overview of the U.S. JGOFS Bermuda Atlantic Time-series Study
546 and the Hydrostation S program. *Deep Sea Research Part II: Topical Studies in Oceanography*, **43**,
547 157–198.
- 548 Nakamura, Y., Itagaki, H., Tuji, A., Shimode, S., Yamaguchi, A., Hidaka, K., and Ogiso-Tanaka, E. (2023)
549 DNA metabarcoding focused on difficult-to-culture protists: An effective approach to clarify biological
550 interactions. *Environmental Microbiology*, **25**, 3630–3638.
- 551 Nakamura, Y. and Suzuki, N. (2015) Phaeodaria: Diverse marine cercozoans of world-wide distribution.
552 Springer, pp. 223–249.
- 553 Ohman, M. D. (2019) A sea of tentacles: optically discernible traits resolved from planktonic organisms in
554 situ. *ICES Journal of Marine Science*, **76**, 1959–1972.
- 555 Panaïotis, T., Babin, M., Biard, T., Carlotti, F., Coppola, L., Guidi, L., Hauss, H., Karp-Boss, L., et al.
556 (2023) Three major mesoplanktonic communities resolved by in situ imaging in the upper 500 m of the
557 global ocean. *Global Ecology and Biogeography*, **32**, 1991–2005.
- 558 Picheral, M., Colin, S. P., and Irisson, J.-O. Ecotaxa.
- 559 Picheral, M., Guidi, L., Stemmann, L., Karl, D. M., Iddaoud, G., and Gorsky, G. (2010) The Underwater
560 Vision Profiler 5: An advanced instrument for high spatial resolution studies of particle size spectra and
561 zooplankton. *Limnology and Oceanography: Methods*, **8**, 462–473.
- 562 Sogawa, S., Nakamura, Y., Nagai, S., Nishi, N., Hidaka, K., Shimizu, Y., and Setou, T. (2022) DNA
563 metabarcoding reveals vertical variation and hidden diversity of alveolata and rhizaria communities in
564 the western north pacific. *Deep Sea Research Part I: Oceanographic Research Papers*, **183**, 103765.

- 565 Stukel, M. R., Biard, T., Krause, J., and Ohman, M. D. (2018) Large Phaeodaria in the twilight zone: Their
566 role in the carbon cycle. *Limnology and Oceanography*, **63**, 2579–2594.
- 567 Stukel, M. R., Ohman, M. D., Kelly, T. B., and Biard, T. (2019) The roles of suspension-feeding and flux-
568 feeding zooplankton as gatekeepers of particle flux into the mesopelagic ocean in the northeast pacific.
569 *Frontiers in Marine Science*, **6**.
- 570 Suzuki, N. and Not, F. (2015) *Biology and ecology of radiolaria*. Springer, pp. 179–222.
- 571 Swanberg, N. R. and Anderson, O. R. (1981) Collozoum caudatum sp. nov.: A giant colonial radiolarian
572 from equatorial and Gulf Stream waters. *Deep Sea Research Part A. Oceanographic Research Papers*, **28**,
573 1033–1047.
- 574 Takahashi, K., Hurd, D. C., and Honjo, S. (1983) Phaeodarian skeletons: Their role in silica transport to
575 the deep sea. *Science*, **222**, 616–618.
- 576 Whitmore, B. M. and Ohman, M. D. (2021) Zooglider-measured association of zooplankton with the fine-
577 scale vertical prey field. *Limnology and Oceanography*, **66**, 3811–3827.
- 578 Wood, S. N. (2017) *Generalized additive models: an introduction with R*. Second edition. CRC Press/Taylor
579 & Francis Group, Boca Raton London New York.
- 580 Wood, S. N. (2001) mgcv: GAMs and Generalized Ridge Regression for R. **1**.
- 581 Zasko, D. N. and Rusanov, I. I. (2005) Vertical Distribution of Radiolarians and Their Role in Epipelagic
582 Communities of the East Pacific Rise and the Gulf of California. *Biology Bulletin*, **32**, 279–287.